The Prostate 68:766–772 (2008)

Increased Spermine Oxidase Expression in Human Prostate Cancer and Prostatic Intraepithelial Neoplasia Tissues

Andrew C. Goodwin,[1] Sana Jadallah,[2] Antoun Toubaji,[2] Kristen Lecksell,[2] Jessica L. Hicks,[2] Jeanne Kowalski,[1] G. Steven Bova,[2,3] Angelo M. De Marzo,[2,3] George J. Netto,[2] and Robert A. Casero Jr.[1]*

[1]*Department of Oncology, Johns Hopkins University School of Medicine and the Sidney Kimmel Comprehensive Cancer Center at Johns Hopkins, Baltimore, Maryland*
[2]*Department of Pathology, Johns Hopkins University School of Medicine and the Sidney Kimmel Comprehensive Cancer Center at Johns Hopkins, Baltimore, Maryland*
[3]*Department of Urology, Johns Hopkins University School of Medicine and the Sidney Kimmel Comprehensive Cancer Center at Johns Hopkins, Baltimore, Maryland*

BACKGROUND. Inflammation has been strongly implicated in prostate carcinogenesis, but the precise molecular mechanisms linking inflammation and carcinogenic DNA damage are not known. Induction of the polyamine catabolic enzyme, spermine oxidase (SMO) has been linked to increased reactive oxygen species (ROS) and DNA damage in human gastric and lung epithelial cells and suggest direct mechanistic links between inflammation, SMO activity, ROS production, and epithelial carcinogenesis that are likely relevant in prostate cancer.
METHODS. Tissue microarrays consisting of matched normal and diseased specimens from patients diagnosed with prostate cancer, prostatic intraepithelial neoplasia (PIN), or proliferative inflammatory atrophy (PIA), as well as unaffected individuals, were stained for SMO expression and analyzed using image analysis techniques and TMAJ software tools.
RESULTS. Average SMO staining was significantly higher in prostate cancer and PIN tissues compared to patient-matched benign tissues. Benign tissues from prostate cancer, PIN, and PIA patients also exhibited significantly higher mean SMO expression versus tissues from prostate disease-free patients.
CONCLUSIONS. Tissues from patients diagnosed with prostate cancer and PIN exhibit, on average, locally increased SMO expression in regions of prostatic disease and higher overall SMO expression in prostatic epithelial cells compared to healthy individuals. Further studies are warranted to directly examine the role of SMO-produced ROS in prostate carcinogenesis.
Prostate 68: 766–772, 2008.

KEY WORDS: **prostate cancer; prostatic intraepithelial neoplasia; spermine oxidase; tissue microarrays; inflammation**

Andrew C. Goodwin and Sana Jadallah contributed equally to this work.

Grant sponsor: NIH; Grant number: CA098454; Grant sponsor: Patrick C. Walsh Prostate Cancer Research Fund.

*Correspondence to: Robert A. Casero Jr., Sidney Kimmel Comprehensive Cancer Center at Johns Hopkins, Bunting-Blaustein Cancer Research Building, Room 551, 1650 Orleans St, Baltimore, MD 21231. E-mail: rcasero@jhmi.edu

Received 5 November 2007; Accepted 29 November 2007
DOI 10.1002/pros.20735
Published online 26 February 2008 in Wiley InterScience (www.interscience.wiley.com).

INTRODUCTION

Chronic inflammation and concomitant increases in reactive oxygen species (ROS) and oxidative damage are estimated to contribute to the etiology of at least 20% of human cancers; however, the precise molecular links remain to be elucidated [1]. In the prostate, studies suggest widespread asymptomatic prostatitis arising from a multitude of stimuli, including microbial infection and dietary components. Emerging epidemiological, histopathological, and molecular evidence suggests that such inflammation may be associated with the development of putatively preneoplastic proliferative inflammatory atrophy (PIA), as well as prostatic intraepithelial neoplasia (PIN) and prostate cancer. PIA lesions consist of regions of atrophic epithelium exhibiting an elevated proportion of proliferating cells, association with inflammatory cells, and increased expression of the pro-inflammatory enzyme cyclooxygenase-2 (*COX-2*) [2–5]. Morphological transitions and close proximity to areas of PIN, and in some cases carcinoma, lend support to the classification of PIA as a probable precursor to these prostatic diseases [3,6].

Histological features of high-grade PIN, the key precursor to prostate cancer, include increased density and stratification of epithelial cells, enlarged nuclei and nucleoli, increased chromatin density, and disruption of the basal cell layer. Whereas proliferation in benign prostatic tissue is predominantly present in basal cells, high-grade PIN lesions feature increased proliferation at the luminal face of prostatic ducts [6,7]. In contrast to PIA, a number of the clonal genetic alterations characteristic of prostate cancer are detected in PIN patients. These include genetic polymorphisms at the Ribonuclease-L (*RNASEL*) and Macrophage Scavenger Receptor (*MSR1*) loci leading to defective gene products that diminish an individual's ability to respond to viral and bacterial pathogens, respectively. In addition, reduced ability to detoxify ROS can result from ineffective 8-oxoguanine DNA glycosylase-1 (*hOGG1*) variants and silencing by promoter hypermethylation of glutathione *S*-transferase π (*GSTP1*; observed in 70% of PIN lesions and 90% of prostate cancers) [2]. Failure to adequately eliminate toxic ROS has been directly linked to carcinogenesis in mice lacking glutathione peroxidases-1 and -2 (*Gpx1* and *Gpx2* double knockout) that develop higher levels of microflora-associated intestinal inflammation and tumors compared to wild-type animals [8].

Polyamines are ubiquitous, polycationic alkylamines that are absolutely required for eukaryotic cell growth and differentiation. Intracellular concentrations of these alkyl amines, demonstrated to be in the millimolar range, are tightly controlled; the dysregulation of polyamine metabolism in cancer cells has long been recognized as a potential target for chemotherapeutic agents [9–11]. Spermine oxidase (SMO) is a newly characterized member of the mammalian polyamine catabolic pathway that catalyzes the back-conversion of spermine to spermidine, producing 3-aminopropanal and the ROS hydrogen peroxide (H_2O_2) as a toxic byproducts (Fig. 1) [12,13]. We have recently demonstrated that SMO is induced in human gastric and lung epithelial cells by *Helicobacter pylori* infection and the pro-inflammatory cytokine tumor necrosis factor-α (TNF-α), respectively, and that this increase in SMO activity produces sufficient H_2O_2 to cause oxidative DNA damage and apoptosis [14,15]. Based on these findings, we hypothesized that increased H_2O_2 resulting from elevated SMO expression may represent a molecular link between chronic inflammation and carcinogenesis in the prostate.

Tissue microarrays (TMAs) provide the unique ability to evaluate a target of interest *in situ* at the DNA, RNA, or protein level in up to 1,000 tissue biopsies simultaneously [16]. In this study, we utilized a collection of human prostate TMAs that included samples from patients diagnosed with PIA, PIN, and prostate adenocarcinoma (PCa), as well as patient-matched benign prostatic tissue (BPT). In addition, we analyzed normal prostate tissue obtained at autopsy from patients without prostatic disease. We employed immunohistochemical (IHC) staining to evaluate the degree of correlation between the clinical status of tissue specimens and SMO expression levels in order to investigate a potential link between expression of SMO and prostate carcinogenesis.

MATERIALS AND METHODS

Tissues and Tissue Microarrays

This study was approved by our institutional review board. Tissue specimens were obtained from donor autopsies or radical retropubic prostatectomies performed at the Johns Hopkins Hospital. All

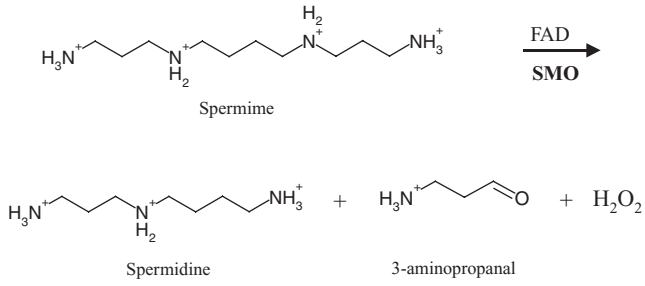

Fig. 1. Spermine oxidase (SMO) enzyme reaction, catalyzing the conversion of spermine to spermidine, 3-aminopropanal, and hydrogen peroxide.

specimens consisted of tissue dissected immediately after surgical removal and immersed in 10% neutral buffered formalin prior to paraffin embedding and processing for IHC. We employed five high-density TMAs to determine the qualitative and quantitative cellular distribution of staining for SMO in PIA, high-grade PIN, and PCa tissues as well as benign tissue from diseased (hereafter ''BPT'') and normal control donor (hereafter ''Normal'') prostates. A total of 879 cores from 94 patients were used for analysis (Table I). TMAs consisted of 0.6 mm tissue cores and were constructed as described previously [17,18].

Immunohistochemistry

A novel rabbit polyclonal antibody raised against human SMO [14] was used for staining control and tissue microarray slides. Manual IHC was performed with the non-biotin based EnVision+ kit (Dako North America, Inc., Carpintaria, CA). Specificity of the antisera was confirmed by blocking the IHC signal with purified SMO as a blocking peptide (not shown). N^1,N^{11},bis(ethyl)norspermine (BENSpm) is known to highly induce SMO in A549 lung cancer cells [19]. Therefore, control and BENSpm-treated A549 cells were imbedded in paraffin and processed identically to the TMA slides and were included as negative and positive controls for each set of TMAs stained.

After paraffin removal and hydration, slides were steamed for 20 min in 10 mM citrate buffer pH 6.0 for antigen retrieval. Endogenous peroxidase was quenched by incubation with peroxidase block for 5 min at room temperature. Slides were incubated with primary antibodies (1:2,000) for 45 min at room temperature. The HRP-conjugated polymer was applied for 30 min, followed by peroxide/diaminobenzidine (DAB) as substrate/chromogen. Slides were then counterstained with Mayer's hematoxylin.

Data Analysis

After SMO staining, TMA slides were scanned using the Bacus Laboratories Image Scanning System (BLISS; Bacus Laboratories, Inc., Lombard, IL). Images were imported into the TMAJ Image application (http://tmaj.pathology.jhmi.edu) as described [20,21]. Histopathological evaluation was performed on each core image by a urologic pathologist, and a final diagnosis was established for each core. Images representing folded, damaged, or non-prostate control tissues were excluded at this stage.

The average intensity and area of staining of each TMA core was calculated using BLISS. To eliminate any potential bias due to variation in the ratio of epithelial to stromal components from core to core, the area of epithelial cytoplasmic staining for SMO was measured in reference to the total area of only the epithelial cells in each core. The latter was determined by adjusting the ''thresholds'' parameters for the *red, green & blue channels* in the BLISS TMA scoring software. The total *''core area threshold''* settings were chosen at the *''core high intensity''* and *''core low intensity''* levels that excluded the maximum stromal component without losing any cytoplasmic measurement. Based on the amount of SMO IHC staining as a percent of the total epithelial tissue area, a SMO expression score (hereafter referred to as ''Percent IHC area'' score) was assigned to each core. Cores containing more than one histological tissue type (i.e., mixed PIA and PCa), as well as cores containing exclusively prostatic stromal tissue were excluded.

Statistical Analysis

SMO staining (mean Percent IHC Area scores) was compared in tissues from patients with and without prostatic disease for each tissue type (Normal vs. BPT, PIA, PIN and PCa; see above) and differences in SMO expression were evaluation by Student's *t*-test.

To compare localized SMO staining in PIA, PIN, and PCa patients, matched pair analyses were conducted for all patients with successfully stained and scored cores representing BPT and one or more additional tissue diagnosis (PIA, PIN, and PCa). This allowed for minimizing the effects of subtle fixation

TABLE I. Distribution of Analyzed Prostate Tissue Cores

	All scored images		Matched pair analysis	
Tissue type	No. of patients	No. of cores	No. of patients	No. of cores
Normal prostate	11	37	n/a	n/a
Benign prostatic tissue	83	483	75	436
Proliferative inflammatory atrophy	25	135	24	134
High-grade prostatic intraepithelial neoplasia	30	82	30	82
Prostate adenocarcinoma	64	142	60	134
Total	94	879	75	786

differences between different specimens that might account for some staining variability. In most cases there were multiple cores from the same patient showing the same diagnosis; therefore, the Percent IHC Area scores for a given diagnosis for a given patient were averaged. Mean PIA, PIN, and PCa SMO staining was calculated relative to BPT for each patient. Differences in relative SMO expression in regions of prostatic disease compared to BPT were evaluated by Student's *t*-test.

RESULTS

SMO expression was analyzed for a total of 879 tissue cores (Table I) as described in Materials and Methods Section. SMO staining was largely confined to epithelial cells and was granular and of cytoplasmic distribution (Fig. 2). We first sought to determine whether overall SMO expression in prostatic epithelial tissues of PIA, PIN, and PCa patients might be elevated compared to individuals without these diseases. Therefore, we assessed SMO expression via immunohistochemical staining of a TMA constructed from control prostate tissue specimens obtained at autopsy from men without detectable prostatic disease (''Normal'' prostatic epithelial tissue). Normal prostatic epithelial tissue exhibited a mean SMO Percent IHC Area score of 27.55 ± 2.21 (mean $\pm$ standard error, $n = 37$ cores). As shown in Figure 3, SMO Percent IHC Area scores in all patient tissues, including BPT (46.56 ± 0.72, $n = 483$), PIA (38.78 ± 1.32, $n = 135$), PIN (57.69 ± 0.63, $n = 82$), and PCa (49.12 ± 1.35, $n = 132$) were significantly higher on average than in Normal control tissue ($P < 0.0001$ for Normal vs. BPT, PIA, PIN, and PCa).

To directly quantify changes in SMO expression in PIA, PIN, and PCa tissues at the level of individual patients while accounting for differences in the number of cores analyzed from each donor, we conducted weighted pairs analyses. SMO staining, measured by average Percent IHC Area scores for each patient's PIA, PIN, or PCa tissue cores and expressed relative to his BPT cores was calculated as described in Materials and Methods Section (Fig. 4). This analysis revealed that mean SMO expression in PIA tissues was 0.81 ± 0.05-fold that of BPT ($n = 24$ patients, $P < 0.01$). In contrast, PIN (1.37 ± 0.1, $n = 30$, $P < 0.01$) and PCa (1.17 ± 0.08, $n = 60$, $P < 0.05$) tissues displayed significantly higher SMO staining than matched BPT. Based on our findings showing higher SMO expression in PIN precursor tissues compared to adenocarcinoma tissues

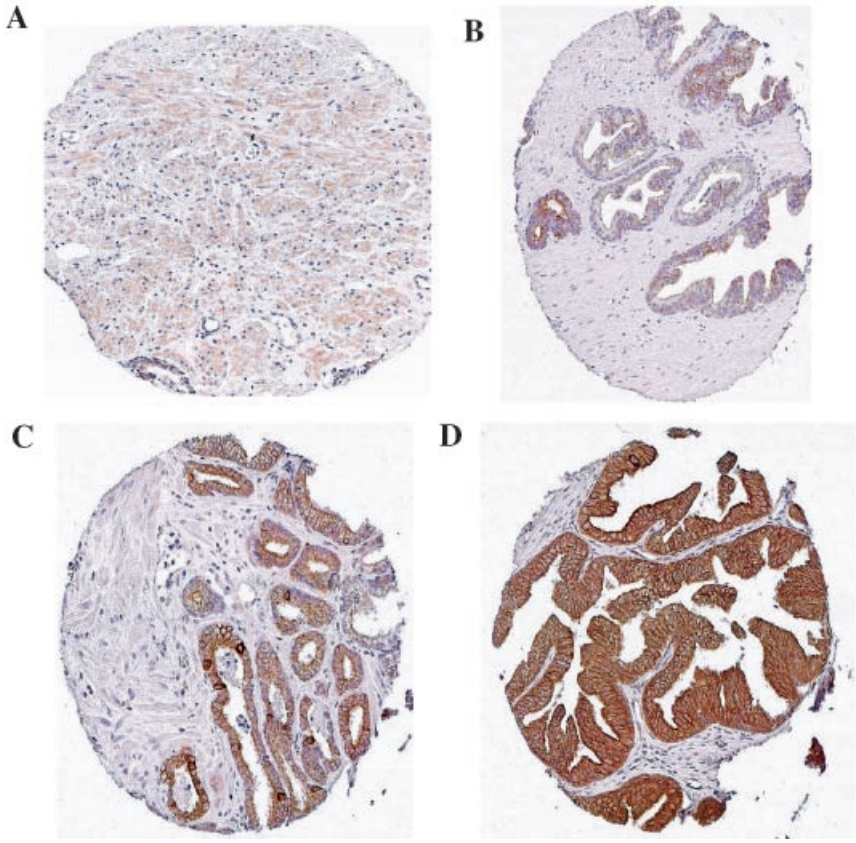

Fig. 2. Representative SMO immunohistochemical staining observed in prostate epithelial tissues. **A**: Normal prostate tissue, (**B**) benign prostate tissue from PCa patient, (**C**) prostate adenocarcinoma, and (**D**) prostatic intraepithelial neoplasia.

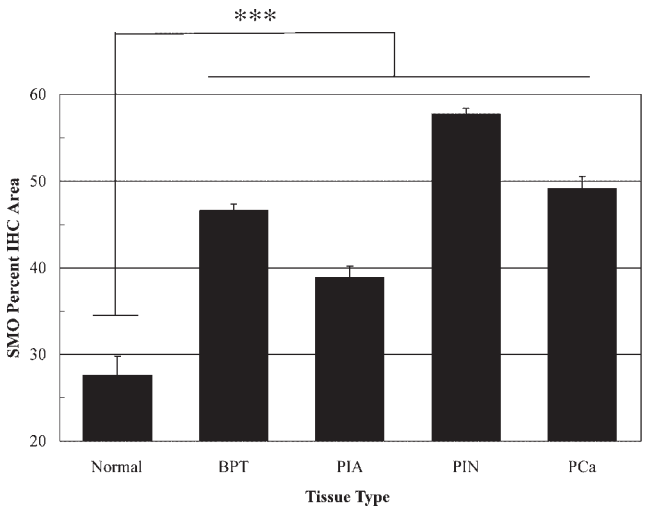

Fig. 3. SMO expression is elevated in prostate tissues of PIA, PIN, and PCa patients. The mean SMO Percent IHC Area score (see Materials and Methods Section) was significantly higher in Benign ("BPT," n = 483), PIA (n = 135), PIN (n = 82), and PCa (n = 142) tissues from patients diagnosed with these prostatic diseases compared to Normal prostatic tissue (n = 37 cores, *** denotes $P < 0.0001$ by Student's *t*-test for all comparisons).

and our hypothesis that SMO induction may play a role in the early stages of the carcinogenic process, we further analyzed SMO levels in PCa tissues based on tumor stage and grade. A trend towards higher SMO staining in lower grade cancers (Gleason Sum <7: 1.27 ± 0.1, n = 40 vs. ≥ 7: 0.97 ± 0.09, n = 20; $P = 0.06$) and earlier stage tumors (T2: 1.24 ± 0.09, n = 45 vs. T3A: 0.95 ± 0.12, n = 14; $P = 0.10$) was observed.

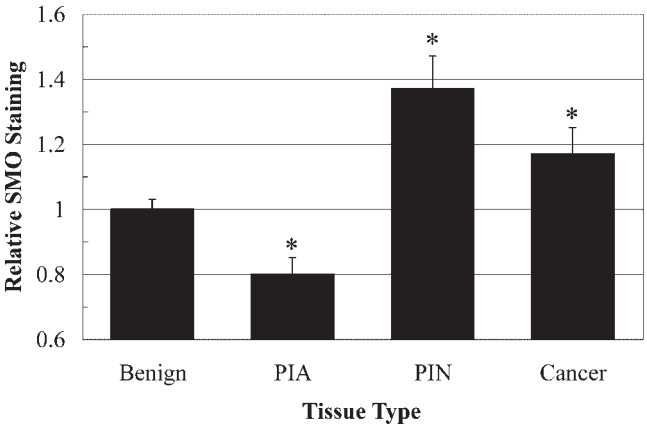

Fig. 4. Matched pair analysis to compare mean differences in SMO expression among tissue types within individual patients. SMO staining (measured by Percent IHC Area scores) is greater in regions of prostatic intraepithelial neoplasia ("PIN", n = 30 patients) or adenocarcinoma ("Cancer", n = 60 patients) and lower in regions of proliferative inflammatory atrophy ("PIA", n = 24 patients) compared to regions of benign prostatic tissue ("Benign"). Differences in mean SMO staining (+standard error), relative to Benign, were evaluated by Student's *t*-test; * denotes $P < 0.05$.

The data presented above clearly demonstrate that PCa and PIN patients exhibit increased SMO staining compared to Normal controls, both in their normal-appearing prostatic epithelial tissue as well as in those regions histologically defined as diseased.

DISCUSSION

Emerging evidence suggests that, as is the case for several other epithelial cancers, chronic inflammation may contribute to the etiology of prostatic intraepithelial neoplasia and prostate adenocarcinoma [2,4,5]. However, the precise molecular mechanisms linking the inflammatory microenvironment to potentially carcinogenic events including DNA damage, tumor suppressor gene inactivation, and increased proliferation remain to be identified. Based on our results in other epithelial models [14,15], we hypothesized that prostatitis-induced SMO expression and its concomitant H_2O_2 production may play a role in the development of proliferative inflammatory atrophy, prostatic intraepithelial neoplasia, and prostate cancer.

In this study, we utilized TMAs as a first step to efficiently analyze SMO expression levels in tissues from 94 patients representing a broad spectrum of prostate pathologies: prostate cancer (PCa), prostatic intraepithelial neoplasia (PIN), proliferative inflammatory atrophy (PIA), benign prostatic epithelium (BPT) from PIA, PIN, and PCa patients, and normal prostate epithelium.

PIA tissues exhibited lower SMO expression than BPT, though further analysis is required to determine whether differences in PIA lesions with respect to degree of immune cell infiltration, active inflammation, or other variables are related to SMO expression levels. The greatest SMO staining was observed in PIN lesions, while SMO expression in PCa was also significantly greater than in patient-matched benign tissues. These results suggest that SMO activity may play a greater role in the development of precursor PIN lesions and initiation events in prostate carcinogenesis versus contributing to later tumor progression. Additional studies will be needed to conclusively link inflammation-induced H_2O_2 production by SMO to specific tumorigenic events.

While we have demonstrated that SMO staining is locally higher in regions of PIN or cancer in the prostate, our data also indicate that patients that developed these prostatic diseases had substantially higher SMO expression in their normal-appearing prostate epithelial areas (BPT) within prostatectomy specimens compared to specimens from men lacking any prostate disease. Our findings are consistent with a

previous study reporting elevated SMO gene expression in prostate cancer tissues based on expressed sequence tag (EST) analysis [22]. These results suggest that individuals with elevated SMO activity may be at more risk for prostate cancer than those with lower SMO activity and are consistent with the hypothesis that prolonged, moderate induction of SMO activity due to prostatitis or other factors may contribute directly to a microenvironment that fosters carcinogenic events.

In addition to the significance of increased production of H_2O_2 by SMO, the relative ability of an individual to respond to elevated ROS levels and prevent cellular damage also significantly impacts the likelihood of disease progression. Deletion and/or inactivation of genes encoding enzymes involved in the detoxification of H_2O_2 and other oxygen radicals, including glutathione-*S*-transferase π (*GSTP1*) [2,23] and glutathione peroxidase-3 (*GPX3*) [24], have been reported in PIA, PIN, and/or prostate cancer. Consequently, our current results demonstrate the likelihood of both an increase in ROS production and decreased oxidative stress-defense mechanisms occurring early in prostate carcinogenesis. Due to the importance of oxidative damage in inflammation-associated epithelial carcinogenesis, inhibition of SMO activity and/or induction of ROS detoxifying enzymes would appear to be attractive targets for chemopreventive therapy.

ACKNOWLEDGMENTS

The authors gratefully acknowledge the assistance of Marianna Zahurak (Department of Oncology, Johns Hopkins). Published TMA images and scoring data are available for online browsing and download at the TMAJ Software Project website of the Johns Hopkins University Tissue Microarray Core Facility (http://tmaj.pathology.jhmi.edu). These studies were supported by NIH grant CA098454 to RAC and the Patrick C. Walsh Prostate Cancer Research Fund, for which RAC is the Schwartz Scholar.

REFERENCES

1. Coussens LM, Werb Z. Inflammation and cancer. Nature 2002; 420(6917):860–867.
2. Nelson WG, De Marzo AM, DeWeese TL, Isaacs WB. The role of inflammation in the pathogenesis of prostate cancer. J Urol 2004; 172(5 Pt 2):S6–S11, discussion; S11–S12.
3. De Marzo AM, Nakai Y, Nelson WG. Inflammation, atrophy, and prostate carcinogenesis. Urol Oncol 2007;25(5):398–400.
4. Platz EA, De Marzo AM. Epidemiology of inflammation and prostate cancer. J Urol 2004;171(2 Pt 2):S36–S40.
5. De Marzo AM, Platz EA, Sutcliffe S, Xu J, Gronberg H, Drake CG, Nakai Y, Isaacs WB, Nelson WG. Inflammation in prostate carcinogenesis. Nat Rev Cancer 2007;7(4):256–269.
6. Montironi R, Mazzucchelli R, Lopez-Beltran A, Cheng L, Scarpelli M. Mechanisms of disease: High-grade prostatic intraepithelial neoplasia and other proposed preneoplastic lesions in the prostate. Nat Clin Pract Urol 2007;4(6):321–332.
7. Joniau S, Goeman L, Pennings J, Van Poppel H. Prostatic intraepithelial neoplasia (PIN): Importance and clinical management. Eur Urol 2005;48(3):379–385.
8. Chu FF, Esworthy RS, Chu PG, Longmate JA, Huycke MM, Wilczynski S, Doroshow JH. Bacteria-induced intestinal cancer in mice with disrupted Gpx1 and Gpx2 genes. Cancer Res 2004; 64(3):962–968.
9. Wang Y, Casero RA Jr. Mammalian polyamine catabolism: A therapeutic target, a pathological problem, or both? J Biochem (Tokyo) 2006;139(1):17–25.
10. Luk GD, Casero RA Jr. Polyamines in normal and cancer cells. Adv Enzyme Regul 1987;26:91–105.
11. Gerner EW, Meyskens FL Jr. Polyamines and cancer: Old molecules, new understanding. Nat Rev Cancer 2004;4(10): 781–792.
12. Wang Y, Devereux W, Woster PM, Stewart TM, Hacker A, Casero RA Jr. Cloning and characterization of a human polyamine oxidase that is inducible by polyamine analogue exposure. Cancer Res 2001;61(14):5370–5373.
13. Vujcic S, Diegelman P, Bacchi CJ, Kramer DL, Porter CW. Identification and characterization of a novel flavin-containing spermine oxidase of mammalian cell origin. Biochem J 2002; 367(Pt 3):665–675.
14. Babbar N, Casero RA Jr. Tumor necrosis factor-alpha increases reactive oxygen species by inducing spermine oxidase in human lung epithelial cells: A potential mechanism for inflammation-induced carcinogenesis. Cancer Res 2006;66(23):11125–11130.
15. Xu H, Chaturvedi R, Cheng Y, Bussiere FI, Asim M, Yao MD, Potosky D, Meltzer SJ, Rhee JG, Kim SS, Moss SF, Hacker A, Wang Y, Casero RA Jr, Wilson KT. Spermine oxidation induced by Helicobacter pylori results in apoptosis and DNA damage: Implications for gastric carcinogenesis. Cancer Res 2004;64(23): 8521–8525.
16. Kononen J, Bubendorf L, Kallioniemi A, Barlund M, Schraml P, Leighton S, Torhorst J, Mihatsch MJ, Sauter G, Kallioniemi OP. Tissue microarrays for high-throughput molecular profiling of tumor specimens. Nat Med 1998;4(7):844–847.
17. Zha S, Gage WR, Sauvageot J, Saria EA, Putzi MJ, Ewing CM, Faith DA, Nelson WG, De Marzo AM, Isaacs WB. Cyclooxygenase-2 is up-regulated in proliferative inflammatory atrophy of the prostate, but not in prostate carcinoma. Cancer Res 2001;61(24):8617–8623.
18. Faith DA, Isaacs WB, Morgan JD, Fedor HL, Hicks JL, Mangold LA, Walsh PC, Partin AW, Platz EA, Luo J, De Marzo AM. Trefoil factor 3 overexpression in prostatic carcinoma: Prognostic importance using tissue microarrays. Prostate 2004;61(3):215–227.
19. Devereux W, Wang Y, Stewart TM, Hacker A, Smith R, Frydman B, Valasinas AL, Reddy VK, Marton LJ, Ward TD, Woster PM, Casero RA. Induction of the PAOh1/SMO polyamine oxidase by polyamine analogues in human lung carcinoma cells. Cancer Chemother Pharmacol 2003;52(5):383–390.
20. Morgan JD, Iacobuzio-Donahue C, Razzaque B, Faith D, De Marzo AM. TMAJ: Open source software to manage a tissue microarray database. 2003; Pittsburgh, PA.
21. De Marzo AM, Morgan JD, Razzaque B, White C, Zimmerman J, Bennett CJ, Fedor H, Faith D. TMAJ: A set of open source software tools to manage a multiple-organ, scalable, secure, multiple-user tissue microarray database. 2002; Pittsburgh, PA.

22. Vujcic S, Liang P, Diegelman P, Kramer DL, Porter CW. Genomic identification and biochemical characterization of the mammalian polyamine oxidase involved in polyamine back-conversion. Biochem J 2003;370:19–28.
23. Nakayama M, Gonzalgo ML, Yegnasubramanian S, Lin X, De Marzo AM, Nelson WG. GSTP1 CpG island hypermethylation as a molecular biomarker for prostate cancer. J Cell Biochem 2004; 91(3):540–552.
24. Yu YP, Yu G, Tseng G, Cieply K, Nelson J, Defrances M, Zarnegar R, Michalopoulos G, Luo JH. Glutathione peroxidase 3, deleted or methylated in prostate cancer, suppresses prostate cancer growth and metastasis. Cancer Res 2007;67(17):8043–8050.